The Journal of Engineering

IET International Radar Conference (IRC 2018)

IET Journals
The Institution of Engineering and Technology

FMCW radar and inertial sensing synergy for assisted living

eISSN 2051-3305
Received on 21st February 2019
Accepted on 7th May 2019
E-First on 26th September 2019
doi: 10.1049/joe.2019.0558
www.ietdl.org

Haobo Li[1], Aman Shrestha[1], Francesco Fioranelli[1] ✉, Julien Le Kernec[1,2], Hadi Heidari[1]

[1]*James Watt School of Engineering, University of Glasgow, Glasgow, UK*

[2]*School of Information and Electronics, University of Electronic Science and Technology of China, Chengdu, People's Republic of China*

✉ *E-mail: francesco.fioranelli@glasgow.ac.uk*

Abstract: This study presents preliminary results about the multi-sensory recognition of indoor daily activities and fall detection, to monitor the well-being of older people at risk of physical and cognitive chronic health conditions. Five different sensors, continuous wave (CW) radar, frequency-modulated CW (FMCW) radar, and inertial measurement unit comprising an accelerometer, gyroscope, and magnetometer were used to simultaneously collect data from 20 subjects performing 10 activities. Rather than using all of the available sensors, it is more efficient and economical to select part of them to maximise the classification accuracy and avoid unnecessary computation to process information if it is not salient. Each individual sensor and several sensor combinations are trained with a quadratic-kernel support vector machine classifier. In addition, they are validated with an improved statistical approach, which uses data from unknown participants to test model rather than random cross-validation to verify if the model generalises well for unknown subjects. Furthermore, the most suitable sensor combinations are derived for each specific group of tested subjects selected (e.g. the oldest, youngest, tallest, and shortest sub-groups of participants out of the entire group).

1 Introduction

Due to the fast development of information and communication technology for sensing, data processing, and communication involving 5G [1], ambient assisted living solutions are capable of providing low-latency intelligence sensing-based products, services, and systems [2, 3]. These can support an increasingly ageing population, enabling them to live independently in their homes, and reduce the cost of health care provision.

Falls [4, 5] have been reported to lead to serious consequences. Apart from physical injuries such as hip fractures and head traumas, loss of confidence, and rehabilitation after these, accidents are proven to reduce the life expectancy of affected people [6]. Hence, there is an incentive to develop an automatic reliable fall detection system [7, 8] that would mitigate trauma following a fall by shortening the response time of emergency services after an incident. This system should also be able to monitor and track the daily activities of people at risk, which is also known as human activity recognition [9–11]. The analysis of the activity patterns can provide useful information on the general well-being of people, and any anomalies in these patterns can enable prompt and proactive treatment in the case of worsening conditions.

Different sensing modalities have been proposed and implemented to achieve the following two targets: human activity classification and fall detection. These involve wearable sensors [11, 12], ambient sensor systems [13, 14], computer vision systems [15], and active/passive radio frequency systems [16, 17].

To select the most suitable ones, the pros and cons of every sensing technologies have to be taken into account in the context of validation accuracy, avoidance of false alarms, the ratio of missed events, response delay, power consumption, computation load, cost, and user acceptance. It is interesting to extract data from different types of sensors, exploit information fusion to combine the advantages of each sensing approach, and complement one with another [18, 19].

Wearable sensors including the inertial measurement unit (IMU) [3], barometric pressure sensor, and global positioning system are widely used in human motion monitoring, because they are easily miniaturised and have a long battery life. However, they need to be placed and worn on different parts of the body (e.g. thigh, wrist, waist, and ankle). Some users may feel discomfort being constrained with wearing a device in their daily life, or simply forget to wear, or to use it properly, especially for cognitively impaired people. Since computer vision systems (video cameras or Kinect) collect plain images of the participants, they invade privacy, especially in private homes (bathroom, toilet, and bedrooms). From a legal standpoint, this might raise issues with image rights that end users and tech investors want to avoid.

Ambient sensor systems are unable to extract the fine-grained information as other sensing techniques can for the purpose of activity classification. Furthermore, retrofitting for large facilities (i.e. smart floors) may not be feasible, which would not be economically viable. Here, an alternative non-intrusive sensing approach with a radar, combined with wearable sensors to provide better overall performance and overcoming the shortcomings of standalone systems, is chosen.

In this paper, we expand our results from [20] with feature-level fusion between all the inertial sensors (accelerometer, gyroscope, and magnetometer) and radar, in which a more realistic statistical approach has been proposed to validate the robustness of the different sensor combinations. It is closer to a realistic scenario, as it keeps data from a sub-group of participants (in this case, one to six participants were left out) for the classifier tests pre-trained with data from different participants. This differs from the common random partitioning of training and testing sets. Furthermore, the optimal sensor combinations for four groups of participants used for testing the classification algorithm were investigated: oldest, youngest, tallest, and shortest out of the 20 subjects.

Section 2 describes the experimental setup and data collection. Section 3 presents raw data pre-processing and feature extraction. Section 4 evaluates the robustness of different sensor combinations by 'leaving one to six subjects out' tests, and subsequent improvements in classification accuracy by sensor fusion. Finally, conclusions and future research directions are discussed in Section 5.

2 Experimental setup and data collection

Data were simultaneously acquired by two software-defined radar and one wearable sensor. They were then exploited through signal processing for feature extraction and activity classification. Radar systems included a frequency-modulated continuous wave

Fig. 1 *Experimental setups with radar and antennas (left) and participant with wearable device at wrist (right)*

Table 1 Inertial sensor specifications

Sensor name	Resolution	Range
accelerometer	490 μg	±16 g
gyroscope	0.06°/s	±2000°/s
magnetometer	0.3 μT	±1300 μT

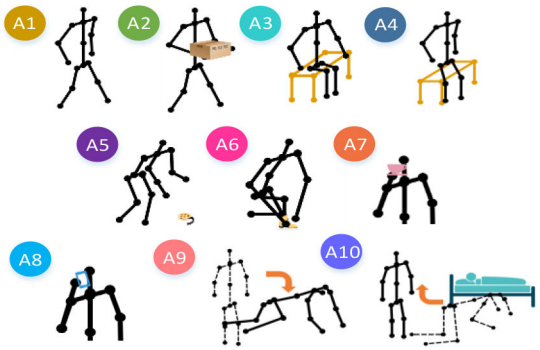

Fig. 2 *Ten activities of daily living performed by participants*

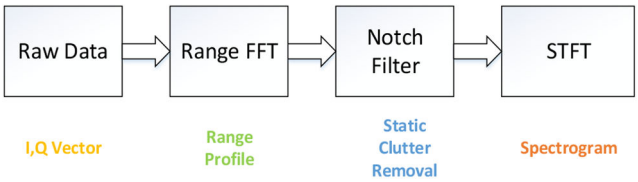

Fig. 3 *Block diagram of radar signal processing*

(FMCW) radar working at 5.8 GHz with 400 MHz bandwidths and 1 ms chirp duration. The wearable sensor comprised a high sensitive tri-axial accelerometer, a gyroscope, and a magnetometer sampling at 50 Hz.

The data collection was performed at the Communication, Sensing and Imaging Laboratory of the University of Glasgow. The experimental setup in Fig. 1 shows the radar system (left) with its antennas on the two tripods, and one of the participants with the wearable sensor on his wrist (right). The radar had a line of sight to the participants, with a distance of ∼1.5–2.5 m. The wearable device (Table 1) was placed on the wrist of the participant dominant hand with a strap. Two vertical polarised Yagi antennas (17 dBi) as part of the radar transceiver antennas were 1.2 m above ground with 30 cm separation. The transmitted power was 19 dBm.

The dataset includes 20 male subjects, aged from 21 to 34 years. Each subject performed 10 different activities (Fig. 2) repeated three times: walk (A1), walk while carrying an object (A2), sitting (A3), standing (A4), pick up an object (A5), tie shoelaces (A6), drink water (A7), answer a phone call (A8), fall (A9), crouch and stand back up (A10). To make the classification more challenging, activities were chosen to be similar, e.g. actions with strong vertical acceleration to the floor, which is easy to confuse with falling.

The raw data can be represented by an $m \times n$ matrix, where m is the number of observations equal to 600 (20 subjects, 10 activities, and 3 repetitions) and n is the number of degrees of freedom (DOFs) equal to 10 (nine from the wearable sensor and one from the radar). The wearable device includes three DOFs for each sensor for X-, Y-, and Z-axis for the accelerometer, gyroscope, and magnetometer. For a given sensor, the data from these three different axes are combined. So, four sensors are used in this paper: accelerometer, gyroscope, magnetometer, and radar.

3 Signal pre-processing and feature extraction

3.1 Radar system

The FMCW radar's raw data (I and Q) pre-processing (Fig. 3) comprises a fast Fourier transform (FFT) to derive the range information. A moving target indicator is then applied to remove static objects to help characterise the different actions of interest with more contrast [21].

Short time Fourier transform across time (0.2 s windows) generates spectrograms slices with the 95% overlap. Movements of different body parts (e.g. arm, torso, limb, and hand) will have distinctive patterns, because of the micro-Doppler effect [22].

Features were extracted from spectrograms and sorted into image textural and physical features (Table 2). The most salient feature is the Doppler frequency centroid, which represents the centre of mass of the movements of the torso and the limbs, and is given by [23]

$$f_c(j) = \frac{\sum_i f(i) S(i,j)}{\sum_i S(i,j)} \tag{1}$$

where $\boldsymbol{S}(i,j)$ denotes the spectrogram matrix and $\boldsymbol{f}(i)$ represents the Doppler frequency of the ith Doppler bins. The bandwidth is also a salient feature, expressed as the Doppler spread around the centre of mass, which is correlated with the range of movements, especially from limbs. It can be derived as follows, where $\boldsymbol{f}_c(j)$ is the centroid at the jth time bin [23]:

$$\boldsymbol{B}_c(j) = \sqrt{\frac{\sum_i (f(i) - f_c(j))^2 S(i,j)}{\sum_i S(i,j)}} \tag{2}$$

Singular value decomposition has been implemented to discover more useful information containing spectral projection of the time and frequency domains, respectively. Other features including skewness and entropy are utilised to give a metric of grey levels of the spectrograms. The cadence velocity diagram is obtained with an FFT across time on the spectrogram to generate the time-localisation info, where the step repetition frequencies (upper and lower) are used as features [24].

Table 2 Features list from the radar sensor

Radar features	#
entropy of spectrogram	1
skewness of spectrogram	1
centroid of spectrogram (mean and variance)	2
bandwidth of spectrogram (mean and variance)	2
singular Value Decomposition (mean and variance of right and left vectors)	12
energy curve of spectrogram	3
step repetition frequency	1
step repetition frequency band peak	2
total	24

Table 3 Features list from the inertial sensor

Time domain	#	Frequency domain	#
norm of XYZ	1	spectral power	9
mean	3	sum of FFT	3
STD	3	coefficients spectral entropy	3
autocorrelation (mean, STD)	6	—	—
cross-correlation (mean, STD)	6	—	—
variance	3	—	—
RMS	3	—	—
MAD	3	—	—
inter-quadrature range	3	—	—
minimum	3	—	—
25th percentile	3	—	—
75th percentile	3	—	—
skewness	3	—	—
kurtosis	—	—	—
total	49	Total	15

Abbreviations: STD, standard deviation; RMS, root mean square; MAD, median absolute deviation

3.2 Inertial measurement unit

Before feature extraction, raw signals recorded from the IMU sensor are band-pass filtered (0.4, 25) Hz. This selects the useful component of the signal from human activities, by eliminating noise close to DC and at higher frequencies due to vibration and bias components within the sensor.

Handcrafted features in the form of numerical parameters, inspired from the literature [9, 25] and previous work [20], were extracted from the processed sensor data. Each individual inertial sensor contributes with 64 features, 192 in total for the accelerometer, gyroscope, and magnetometer (Table 3).

Features have been divided into the time and frequency domains. In the time domain, typical statistical parameters involving mean, variance, standard deviation (STD), skewness, and kurtosis [16] are used. A cross-correlation is considered to distinguish activities with body dimension change. Spectrum features contain spectral power at three specific frequency bands, in particular, 0.5–1, 1–5, and 5–10 Hz, spectral entropy of the normalised power density function, the power spectrum density, and the cumulative sum of the absolute value of FFT indices.

Considering 64 features from each inertial sensor, and 24 features from the FMCW radar, 216 feature samples are used for sensor fusion and classification. Through a feature selection method presented in [24], optimal feature combinations can be generated, enabling higher classification accuracy with fewer features. However, this task is computationally intensive for all the considered scenarios; thus, in this paper, we will only consider fusion for simplicity. Feature selection will be conducted in further work.

Prior to the classification, features generated by the processed data were normalised by subtracting the mean and dividing by the STD, in order to make the values of each feature vector with the zero mean and unit variance.

Table 4 Lists of sensors combination for fusion

1 sensor	Accelerometer	Gyroscope	Magnetometer	Radar
fusion of two sensors	accelerometer and radar			
	gyroscope and radar			
	magnetometer and radar			
fusion of three sensors	accelerometer, gyroscope, and radar			
	accelerometer, gyroscope, and magnetometer			
fusion of all sensors	accelerometer, gyroscope, magnetometer, and radar			

4 Classification and feature fusion results

Quadratic-kernel support vector machine (SVM) [26] is used as a classifier. Typically, SVM is used for separating data into binary classes by maximising the margin, which is determined as the distance between the hyperplane and the closest data point at either side of the feature space. The set of specific points close to the decision boundary that defines the margin offset is known as support vectors, as they also define the hyperplane. This hyperplane and the consequent minimisation function could be expressed as follows [27]:

$$f = x'\boldsymbol{\beta} + b \tag{3}$$

$$\min_{\beta,\beta_0} \frac{1}{2}\| \boldsymbol{\beta} \|^2 + C\sum_{i=1}^{n} \xi_i \tag{4}$$

where $\boldsymbol{\beta}$ is the normal vector to the hyperplane and b is the bias coefficient. C ($C > 0$) is a penalty factor, which determines soft or hard margins in terms of the tolerance of allowing data points at the wrong side. The larger the C, the narrower the margin and vice versa. C should be carefully chosen to prevent underfitting or overfitting. Our penalty factor in the SVM training is set as 1. ξ_i ($\xi_i \geq 0$) is the slack variable (classification error relative to the hyperplane). Data points between the margin and hyperplane will be allocated a slack variable from 0 to 1, depending on the distance to the hyperplane. In the case of misclassification, the slack variable is >1. If a linear separation margin in the given space is not present, a kernel function is used to map feature samples to a higher dimension where a linear boundary is present [26]. Choices for the kernel are based on the desired hyperplane, such as Gaussian, cubic, and quadratic to mention a few.

SVM can be implemented for multi-class problems by combining a multiple binary SVM. To distinguish the 10 classes, 45 binary SVMs were needed to separate all classes from one another, and these were implemented in MATLAB.

Information fusion implies to combine data from different sources or sensors, which could be performed at the signal, feature, or decision level. We consider feature-level fusion to provide improved accuracy and reduce false alarms and false positives between activities. The sensor combinations are listed in Table 4, with the aim of evaluating whether good classification accuracy can be achieved without using a reduced sensor suite with the added bonus of a reduced computational load.

Generally, 'Holdout' and 'K-fold' are the two most common ways to divide the available data into training and validation sets.

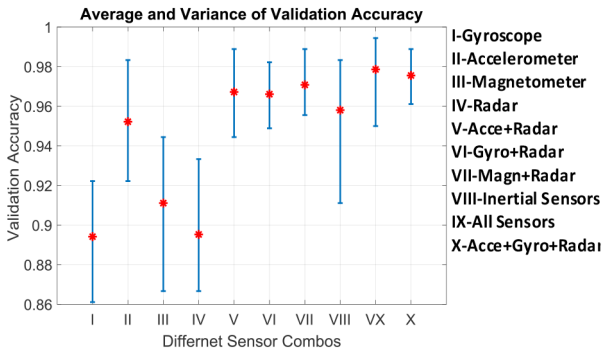

Fig. 4 *Average and min–max range of classification accuracy for 20 iteration Holdout*

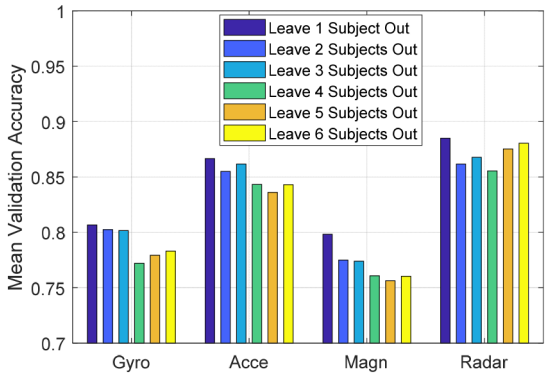

Fig. 5 *Mean classification accuracy for individual sensors for 'leaving one to six subjects out'*

Holdout divides the data randomly into two parts according to a defined ratio: one part for training the classifier and the other for testing. Holdout requires multiple tests to be averaged, since it may select 'good' or 'bad' parts of data in a biased manner, thereby generating high- or low-classification accuracy not reflecting the actual classification performance. K-fold distributes the data in K sub-sets, and each one is used to test the classifier, while the others are used for training; the final result is the average value of K tests.

Operationally, the pre-trained classifier will never see the data from the unknown participants before testing; thus, it is more realistic to validate the robustness of classifiers by 'leaving one or more participants out'. This cross-validation approach is different from Holdout and K-fold; the data are not randomly partitioned into training and testing sets. Instead, data from one participant are separated and used to test the classifier, which is trained with data from the other subjects. The whole process is repeated and averaged for all participants.

In this paper, the number in the 'left-out' groups for testing varied from one to six subjects, randomly chosen to test the robustness of the classifier with more 'unknown' subjects. Furthermore, we also selected the specific four 'left-out' subjects, oldest, youngest, tallest, and shortest, out of the 20 participants. For each sub-group, two subjects at a time are used as the test set, repeating the process six times to test all combinations. Different sensor combinations were tried for each sub-group, and the most suitable combinations were identified comparing the average classification accuracy.

Table 5 shows the 'leave subjects out' cross-validation methods used in this paper with the corresponding training-testing ratio. Holdout with the 7:3 ratio is used as a baseline to compare the performance of each sensor's combination.

4.1 Analysis and discussion of the results

Fig. 4 shows the average and min–max range of test classification accuracies for different sensor combinations obtained by running 20 iterations of Holdout. The accelerometer yields the best classification performance in the single-sensor case. However, integration with any other sensor significantly improves the mean accuracy and reduces variance. Accuracy increases from 1 to 1.5% when other sensors are added.

Table 5 Lists of cross-validation methods used in this work

Cross-validation methods	Training and testing ratio
holdout	30–70%
leave one to six subjects out	5–95% (one subject)
	10–90% (two subjects)
	15–85% (three subjects)
	20–80% (four subjects)
	25–75% (five subjects)
	30–70% (six subjects)
sub-group: oldest people	10–90%
sub-group: youngest people	10–90%
sub-group: tallest people	10–90%
sub-group: shortest people	10–90%

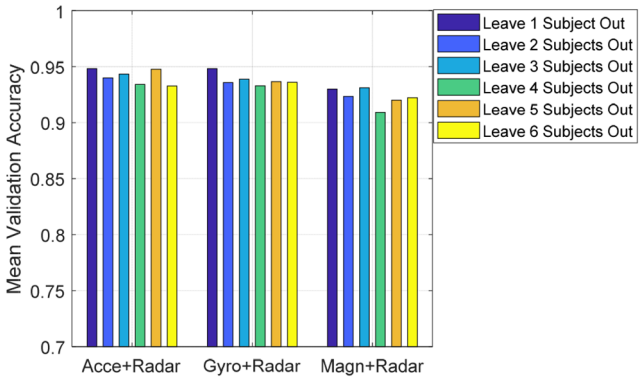

Fig. 6 *Mean classification accuracy for 'leaving out one to six subjects' (two sensor fusion)*

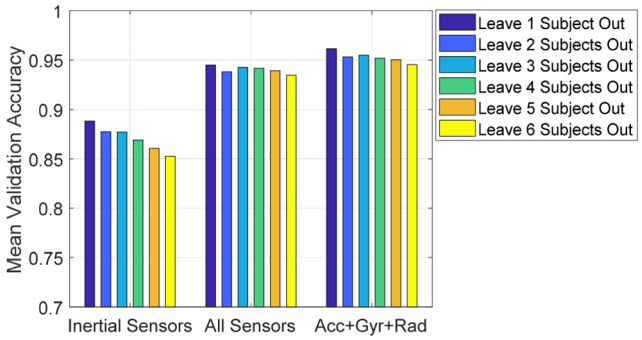

Fig. 7 *Mean classification accuracy for 'leaving out one to six subjects' (multiple sensors)*

Figs. 5–7 present 'leaving one to six subjects out' tests for individual sensors, fusion of two sensors, and fusion of three or all sensors. The radar outperforms other individual sensors, followed by the accelerometer and gyroscope, whereas the magnetometer has the worst performance. If the features from one inertial sensor are combined with the radar, the mean classification accuracy increases by 6–13% compared to using a single sensor. The fusion of all sensors did not show much improvement compared with the radar plus one sensor. The two best wearable sensors, the accelerometer and the gyroscope, were selected to integrate with the radar, yielding the highest mean accuracy (~95%) in 'leaving one to six subjects out' tests.

Compared to the general Holdout test in Fig. 4, this 'leaving one to six subjects out' test produces worse classification accuracy in each sensor combination, e.g. radar (2%), single inertial sensor (10%), and sensor fusion (3%). For the best combination (accelerometer + gyroscope + radar), the reduction in accuracy is ~3%. A diminished performance was expected, as leaving out data challenges the classifier.

Table 6 Minimum classification accuracy of 'leaving out one to six subjects' test

Sensors combinations	No of subjects left out					
	1	2	3	4	5	6
gyroscope	0.47	0.57	0.56	0.66	0.66	0.62
accelerometer	0.7	0.7	0.76	0.73	0.76	0.79
magnetometer	0.4	0.53	0.57	0.72	0.66	0.63
radar	0.7	0.68	0.79	0.8	0.82	0.82
accelerometer + radar	0.8	0.83	0.88	0.88	0.91	0.89
gyroscope + radar	0.77	0.8	0.87	0.84	0.89	0.87
magnetometer + radar	0.67	0.78	0.84	0.83	0.88	0.85
inertial sensor	0.7	0.65	0.74	0.79	0.76	0.74
all sensors	0.7	0.8	0.84	0.9	0.9	0.88
acce + gyro + radar	0.8	0.82	0.87	0.9	0.91	0.9

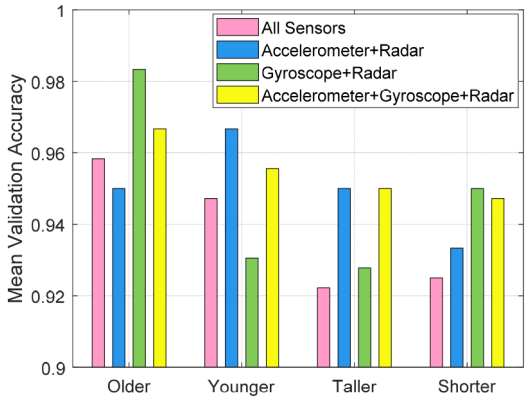

Fig. 8 *Accuracy for different sensor combinations for specific testing sub-groups*

Table 7 Confusion matrix of general Holdout

%	A1	A2	A3	A4	A5	A6	A7	A8	A9	A10
A1	**100**	—	—	—	—	—	—	—	—	—
A2	—	**100**	—	—	—	—	—	—	—	—
A3	—	—	**99.1**	—	—	—	—	—	—	*0.9*
A4	—	—	*0.6*	**97.8**	*0.8*	—	—	*0.8*	—	—
A5	—	—	*2.6*	1.3	**93.2**	*1.0*	—	*0.8*	—	*1.0*
A6	—	—	—	—	—	**97.8**	—	—	*2.2*	—
A7	—	—	—	—	—	—	**99.2**	*0.8*	—	—
A8	—	—	—	—	*0.6*	—	*1.7*	**96.7**	—	*1.0*
A9	—	—	*0.3*	—	—	*0.3*	—	—	**99.4**	—
A10	—	—	*1.1*	—	—	—	—	—	—	**98.9**

Besides the mean accuracy, the minimum accuracy of the 20 iterations with one to six subjects left out is shown in Table 6. The minimum is a measure of the worst classification performance for an unknown subject. The highest minima are highlighted in bold. The accelerometer provides the best 'worst accuracy' of the three inertial sensors. For inertial sensors combined with the radar, the minimum accuracy increases, thanks to sensor fusion, with 'accelerometer + gyroscope + radar' and 'accelerometer + radar' outperform the other options providing the minimum accuracy of 90%.

Fig. 8 introduces the results from testing the sensitivity of the classification accuracy against two attributes: age and height. This results in four sub-groups: younger versus older people and shorter versus taller people. The classification is ran on one sub-group, e.g. older people leaving two people out of the training set and testing on the two left out. This obtained accuracy is the average of the six iterative tests of all combinations. It is interesting to observe that 'gyroscope + radar' and 'accelerometer + radar' sensor combinations, outperform other sensor combinations for the older and younger groups, respectively, whereas the combination 'accelerometer + gyroscope + radar' indicates the best generalised performance among the tallest and shortest participants. This appears to show that the best combination of sensors can be affected by the user group and that optimal sensor fusion should consider the target population characteristics (in our case, the elderly) in the specific scenario to maximise accuracy, as this has an incidence on performance. Two significant factors, notably age and height, were found to influence the classification performance, especially in the likelihood of fall events. In Fig. 8, older people classification performed better than younger people classification; however, the 'older people' in our dataset have an age range from 28 to 35, which is not representative for elderly end users but would indicate that tests on representatives of the target age group for the classification are primordial to minimise false alarms. The outcomes of testing on taller and shorter groups decrease ∼3–5% compared to the general Holdout, which means that height and body types also need to be taken into account.

Tables 7 and 8 show the confusion matrices for general Holdout and 'leave one participants out' tests, considering the best sensor combination 'accelerometer + gyroscope + radar'. The green diagonal indicates the correctly classified actions, whereas the non-diagonal elements highlighted with yellow are the missed classification (horizontal) and false alarms (vertical) corresponding to each class. In Table 7, the most significant event A9, fall, is almost 100% correctly classified with little misclassification with sitting down and tying shoelaces. The results decreased in Table 8

Table 8 Confusion matrix of 'leaving one participant out' test

%	A1	A2	A3	A4	A5	A6	A7	A8	A9	A10
A1	**100**	—	—	—	—	—	—	—	—	—
A2	—	**100**	—	—	—	—	—	—	—	—
A3	—	—	**93.3**	*1.7*	*3.3*	—	—	—	—	—
A4	—	—	—	**100**	—	—	—	—	—	—
A5	—	—	—	*3.3*	**93.3**	—	—	*3.3*	—	—
A6	—	—	—	—	*3.3*	**95**	—	—	*1.7*	—
A7	—	—	—	—	*1.7*	—	**93.3**	*5*	—	—
A8	—	—	—	*1.7*	—	—	*3.3*	**95**	—	—
A9	—	—	—	—	—	*3.3*	—	*1.7*	**95**	—
A10	—	—	—	—	*1.7*	—	—	—	—	**98.3**

as expected, especially for the groups (A3 sitting and A4 standing) and (A5 picking up an object, A7 drinking water, and A8 answering the phone) which were deliberately chosen to be similar to each other to set up a challenging classification problem.

5 Conclusions

In this paper, we have demonstrated that fusion between heterogeneous sensors improves the classification accuracy and presented an improved validation method, where the data used to test the trained classifier are from several unknown participants, 'left out' at the training stage. The most suitable sensor combination for each special group is derived through dividing the participants into sub-groups.

For further research directions, more data, including more elderly people, more female subjects, more sensor sources in terms of different operating bands of radar and commercial WIFI hotspot [17], will be considered. More data fusion techniques could also be explored to provide subsequent improvement, involving signal-level fusion with multiple sensor sources using a Kalman filterm decision-level fusion of posterior possibility within the logP algorithm [28] and voting system [29]. Meanwhile, better feature combinations could be generated to reduce the computational loads and maximise the classification accuracy with filter methods (e.g. F-score, Relief-F, and principal component analysis) or time-consuming wrapper method (e.g. sequential forward selection) or embedded method which integrates classification with feature selection (e.g. SVM recursive feature elimination) [30].

6 Acknowledgments

The author are grateful to all the participants to the data collection. The author acknowledges support from the UK EPSRC through grant EP/R041679/1 INSHEP, and Doctoral Training Award supporting A. Shrestha in his PhD at the School of Engineering, University of Glasgow.

7 References

[1] Mumtaz, S., Bo, A., Al-Dulaimi, A., *et al.*: '5G and beyond mobile technologies and applications for industrial IoT (IIoT)', *IEEE Trans. Ind. Inf.*, 2018, **99**, pp. 1–1

[2] Erden, F., Velipasalar, S., Alkar, A.Z., *et al.*: 'Sensors in assisted living: a survey of signal and image processing methods', *IEEE Signal Process. Mag.*, 2016, **33**, (2), pp. 36–44

[3] Bennett, T.R., Wu, J., Kehtarnavaz, N., *et al.*: 'Inertial measurement unit-based wearable computers for assisted living applications: a signal processing perspective', *IEEE Signal Process. Mag.*, 2016, **33**, (2), pp. 28–35

[4] U. D. O. Health and H. Services: 'Report to Congress: aging services technology study', Washington, DC, 2012

[5] Terroso, M., Rosa, N., Marques, A.T., *et al.*: 'Physical consequences of falls in the elderly: a literature review from 1995 to 2010', *Eur. Rev. Aging. Phys. Act.*, 2014, **11**, (1), p. 51

[6] World Health Organisation: 'WHO global report on falls prevention in older age', Ageing and Life Course, Family and Community Health Report, WHO Press, Geneva, Switzerland, 2008, pp. 6–12

[7] Chen, J., Kwong, K., Chang, D., *et al.*: 'Wearable sensors for reliable fall detection'. IEEE-EMBS 2005, 27th Annual Int. Conf. of the Engineering in Medicine and Biology Society, Shanghai, China, September 2005, pp. 3551–3554

[8] Mubashir, M., Shao, L., Seed, L.: 'A survey on fall detection: principles and approaches', *Neurocomputing*, 2013, **100**, pp. 144–152

[9] Chernbumroong, S, Atkins, A.S., Yu, H.: 'Activity classification using a single wrist-worn accelerometer'. 5th Int. Conf. on Software, Knowledge Information, Industrial Management and Applications (SKIMA), Benevento, Italy, 2011, pp. 1–6

[10] López-Nava, I.H., Muñoz-Meléndez, A.: 'Wearable inertial sensors for human motion analysis: a review', *IEEE Sens. J.*, 2016, **16**, (22), pp. 7821–7834

[11] Mukhopadhyay, S.C.: 'Wearable sensors for human activity monitoring: a review', *IEEE Sens. J.*, 2015, **15**, (3), pp. 1321–1330

[12] Patel, S., Park, H., Bonato, P., *et al.*: 'A review of wearable sensors and systems with application in rehabilitation', *J. Neuroeng. Rehabil.*, 2012, **9**, (1), p. 21

[13] Rajendran, P.J.: 'A smart and passive floor-vibration based fall detector for elderly'. 2nd Int. Conf. on Information & Communication Technologies, Damascus, Syria, 2006

[14] Tao, S., Kudo, M., Nonaka, H.: 'Privacy-preserved behavior analysis and fall detection by an infrared ceiling sensor network', *Sensors*, 2012, **12**, (12), pp. 16920–16936

[15] Cippitelli, E., Fioranelli, F., Gambi, E., *et al.*: 'Radar and RGB-depth sensors for fall detection: a review', *IEEE Sens. J.*, 2017, **17**, (12), pp. 3585–3604

[16] Shrestha, A., Le Kernec, J., Fioranelli, F., *et al.*: 'Feature diversity for fall detection and human indoor activities classification using radar systems'. Int. Conf. on Radar Systems (Radar 2017), Belfast, UK, 2017

[17] Wang, H., Zhang, D., Wang, Y., *et al.*: 'RT-Fall: a real-time and contactless fall detection system with commodity WiFi devices', *IEEE Trans. Mob. Comput.*, 2017, **16**, (2), pp. 511–526

[18] Castanedo, F.: 'A review of data fusion techniques', *Scientific World J.*, 2013, **2013**, pp. 1–19

[19] Castro, I.D., Mercuri, M., Torfs, T., *et al.*: 'Sensor fusion of capacitively-coupled ECG and continuous-wave Doppler radar for improved unobtrusive heart rate measurements', *IEEE J. Emerg. Selected Top. Circuits Syst.*, 2018, **PP**, (99), pp. 1–1

[20] Li, H., Shrestha, A., Fioranelli, F., *et al.*: 'Multisensory data fusion for human activities classification and fall detection'. Proc. of IEEE Sensors, Glasgow, UK, October 29–31 2017, pp. 909–911

[21] Fioranelli, F., Ritchie, M., Griffiths, H.: 'Classification of unarmed/armed personnel using the NetRAD multistatic radar for micro-Doppler and singular value decomposition features', *IEEE Geosci. Remote Sens. Lett.*, 2015, **12**, (9), pp. 1933–1937

[22] Chen, V.C., Miceli, W.J., Tahmoush, D.: '*Radar micro-Doppler signatures: processing and applications*' (The Institution of Engineering and Technology, London, UK, 2014)

[23] Fioranelli, F., Ritchie, M., Griffiths, H.: 'Centroid features for classification of armed/unarmed multiple personnel using multistatic human micro-Doppler', *IET Radar Sonar Navig.*, 2016, **10**, (9), pp. 1702–1710

[24] Zhu, J., San-Segundo, R., Pardo, J.M.: 'Feature extraction for robust physical activity recognition', *Hum.-centric Comput. Inf. Sci.*, 2017, **7**, (1), p. 16

[25] Li, H., Shrestha, A., Heidari, H., *et al.*: 'A multi-sensory approach for remote health monitoring of older people', *IEEE J. Electromagn., RF Microw. Med. Biol.*, 2018, **2**, pp. 1–1

[26] Cortes, C., Vapnik, V.: 'Support-vector networks', *Mach. Learn.*, 1995, **20**, (3), pp. 273–297

[27] Bufler, T.D., Narayanan, R.M.: 'Radar classification of indoor targets using support vector machines', *IET Radar Sonar Navig.*, 2016, **10**, (8), pp. 1468–1476

[28] Chen, C., Jafari, R., Kehtarnavaz, N.: 'A real-time human action recognition system using depth and inertial sensor fusion', *IEEE Sens. J.*, 2016, **16**, (3), pp. 773–781

[29] Gibson, R.M., Amira, A., Ramzan, N., *et al.*: 'Multiple comparator classifier framework for accelerometer-based fall detection and diagnostic', *Appl. Soft Comput.*, 2016, **39**, pp. 94–103

[30] Roffo, G.: 'Feature selection library (MATLAB toolbox)', arXiv preprint arXiv:1607.01327, 2016